The Plant Cell, Vol. 17, 486–501, February 2005, www.plantcell.org © 2005 American Society of Plant Biologists

Arabidopsis VILLIN1 Generates Actin Filament Cables That Are Resistant to Depolymerization

Shanjin Huang,[a] Robert C. Robinson,[b] Lisa Y. Gao,[a] Tracie Matsumoto,[a,2] Arnaud Brunet,[c] Laurent Blanchoin,[c,1] and Christopher J. Staiger[a,1]

[a] Department of Biological Sciences and Purdue Motility Group, Purdue University, West Lafayette, Indiana 47907-2064
[b] Department of Medical Biochemistry and Microbiology, Uppsala University, 751 23 Uppsala, Sweden
[c] Laboratoire de Physiologie Cellulaire Végétale, Commissariat à l'Energie Atomique/Centre National de la Recherche Scientifique/Université Joseph Fourier, F38054 Grenoble, France

Dynamic cytoplasmic streaming, organelle positioning, and nuclear migration use molecular tracks generated from actin filaments arrayed into higher-order structures like actin cables and bundles. How these arrays are formed and stabilized against cellular depolymerizing forces remains an open question. Villin and fimbrin are the best characterized actin-filament bundling or cross-linking proteins in plants and each is encoded by a multigene family of five members in *Arabidopsis thaliana*. The related villins and gelsolins are conserved proteins that are constructed from a core of six homologous gelsolin domains. Gelsolin is a calcium-regulated actin filament severing, nucleating and barbed end capping factor. Villin has a seventh domain at its C terminus, the villin headpiece, which can bind to an actin filament, conferring the ability to crosslink or bundle actin filaments. Many, but not all, villins retain the ability to sever, nucleate, and cap filaments. Here we have identified a putative calcium-insensitive villin isoform through comparison of sequence alignments between human gelsolin and plant villins with x-ray crystallography data for vertebrate gelsolin. VILLIN1 (VLN1) has the least well-conserved type 1 and type 2 calcium binding sites among the Arabidopsis VILLIN isoforms. Recombinant VLN1 binds to actin filaments with high affinity (K_d ~1 μM) and generates bundled filament networks; both properties are independent of the free Ca^{2+} concentration. Unlike human plasma gelsolin, VLN1 does not nucleate the assembly of filaments from monomer, does not block the polymerization of profilin-actin onto barbed ends, and does not stimulate depolymerization or sever preexisting filaments. In kinetic assays with ADF/cofilin, villin appears to bind first to growing filaments and protects filaments against ADF-mediated depolymerization. We propose that VLN1 is a major regulator of the formation and stability of actin filament bundles in plant cells and that it functions to maintain the cable network even in the presence of stimuli that result in depolymerization of other actin arrays.

INTRODUCTION

The actin cytoskeleton is a ubiquitous and dynamic scaffolding that is present in the cytoplasm of eukaryotic cells and plays a central role in numerous physiological processes, including muscle contraction, cell motility, organelle movement, vesicle trafficking, and cytoplasmic streaming. Understanding how the actin cytoskeleton is organized, how its dynamics are regulated, and how its structure and function respond to environmental cues are open questions in cell biology.

In plant cells, actin filaments often form prominent higher-order structures, such as bundles and cables, which serve as tracks for cytoplasmic streaming and organelle movements. A classic example is the actin cables within green algal cells of Nitella and Chara, where up to 100 actin filaments of uniform polarity are packed into a single actin bundle (Nagai and Rebhun, 1966). In several examples from higher plants, such as the root hair cells of Hydrocharis and stamen hair cells of Tradescantia, actin-filament bundles are involved not only in cytoplasmic streaming but also in stabilizing the structure of transvacuolar strands and maintaining the overall cellular architecture (Staiger et al., 1994; Shimmen et al., 1995; Valster et al., 1997; Tominaga et al., 2000). It has also been inferred that actin bundles play an important role in nuclear positioning, keeping the nucleus at a fixed distance from the growing root hair tip (Ketelaar et al., 2002). The size, shape, location, and number of actin bundles changes during the development of Drosophila bristles, leading to a suggestion that the status of internal actin bundles relates to morphogenesis (Tilney et al., 2003). Similarly, the presence of filament bundles at particular stages of plant cell growth (Thimann et al., 1992; Waller and Nick, 1997; Waller et al., 2002) and their loss or reduction in mutants of *Arabidopsis thaliana* with defective trichomes (Le et al., 2003; El-Assal et al., 2004) or maize (*Zea mays*) mutants with deficient root cell expansion (Baluska et al., 2001) hint at additional roles during cell elongation and cellular morphogenesis. Bundles of actin also converge upon the

[1] To whom correspondence should be addressed. E-mail cstaiger@bilbo.bio.purdue.edu or laurent.blanchoin@cea.fr; fax 765-496-1496 or 33-4-38785091.
[2] Current address: USDA/ARS Pacific Basin Agricultural Research Center, Pacific Basin Tropical Plant Genetic Resource Management Unit Hilo, HI 96720.
The author responsible for distribution of materials integral to the findings presented in this article in accordance with policy described in the Instructions for Authors (www.plantcell.org) is: C.J. Staiger (cstaiger@bilbo.bio.purdue.edu).
Article, publication date, and citation information can be found at www.plantcell.org/cgi/doi/10.1105/tpc.104.028555.

site of fungal attack in epidermal cells (Kobayashi et al., 1992, 1997; Gross et al., 1993) and are implicated in the nonhost and host cell responses to pathogens (reviewed in Staiger, 2000; Schmelzer, 2002).

Specific families of actin binding proteins are thought to be responsible for actin bundle formation in the cell. However, rather little is known about the actin cross-linking and bundling proteins from plant cells when compared with nonplant cells (McCurdy et al., 2001; Wasteneys and Galway, 2003; Staiger and Hussey, 2004). Villin, which was originally isolated from the core actin bundles of intestinal epithelial cell microvilli (Bretscher and Weber, 1979; Matsudaira and Burgess, 1979), is one of the main proteins responsible for actin bundle formation. Villin belongs to a superfamily of actin binding proteins called the villin/gelsolin family (Friederich and Louvard, 1999; Yin, 1999). These are constructed from 125 to 150 amino acid gelsolin-repeat domains. Villin and gelsolin contain six gelsolin repeats (G1–G6), whereas severin, fragmin, and CapG contain three repeats (G1–G3). Gelsolin has Ca^{2+}-stimulated filamentous actin (F-actin) severing activity. Gelsolin also caps the barbed ends of actin filaments and nucleates formation of new filaments. Villin/gelsolin homologs have not been found in the *Saccharomyces cerevisiae* genome. Recently, we isolated an actin binding protein from poppy (*Papaver rhoeas*) pollen, PrABP80; biochemical and microscopic characterization confirmed that it is gelsolin-like (Huang et al., 2004). Examples of the three domain protein have also been isolated from *Lilium davidii* pollen (Fan et al., 2004) and *Mimosa pudica* (Yamashiro et al., 2001), and the authors inferred that these fragmin-like proteins had severing activity.

In addition to a gelsolin-like core domain, villins contain an additional C-terminal actin binding module called the villin headpiece. The headpiece allows each molecule of villin to contact two adjacent filaments and to cross-link filaments into bundles, a property that is missing from gelsolins. In the presence of micromolar Ca^{2+}, most, but not all, villins sever actin filaments and cap filament barbed ends (Glenney et al., 1980; Northrop et al., 1986; Janmey and Matsudaira, 1988). Knockout mice with a null allele for villin have normal intestinal microvilli, but are defective in Ca^{2+}-stimulated fragmentation and destruction of the brush borders, leading to the conclusion that villin is essential for cytoskeletal reorganization in response to stimuli (Ferrary et al., 1999). By contrast, Drosophila mutations in the *Quail* gene lead to female sterility and have defects in actin bundle formation during oogenesis (Mahajan-Miklos and Cooley, 1994; Matova et al., 1999). Although the core gelsolin-homology domains of Quail are highly conserved, the recombinant protein does not sever, cap, or nucleate actin filaments in vitro (Matova et al., 1999). This result emphasizes the need to make direct measurements of the actin binding properties for each villin family member before assuming its function in vivo. Two actin-bundling proteins from lily (*Lilium longiflorum*) pollen tubes, 135-ABP and 115-ABP, were isolated by biochemical fractionation (Yokota et al., 1998), and sequence analyses reveal that both are plant villins (Vidali et al., 1999; Yokota et al., 2003). Although lily villin isoforms bundle actin filaments in a Ca^{2+}/calmodulin dependent manner, they do not have obvious severing or capping activity (Nakayasu et al., 1998; Yokota and Shimmen, 1999; Yokota et al., 2000). The Arabidopsis genome contains sequences for five villin-like genes (VLN1−5; Klahre et al., 2000; Staiger and Hussey, 2004) and GFP–villin fusions associate with actin filaments in vivo (Klahre et al., 2000). However, there is no genetic or biochemical evidence for the function of AtVLNs.

Various actin binding proteins perform in harmony to generate particular F-actin structures; for example, cloud-like networks of dendritically-nucleated actin filaments formed on Arp2/3-coated beads in vitro are converted into filopodia-like bundles in the absence of capping protein (Vignjevic et al., 2003). The side binding protein tropomyosin inhibits Arp2/3-induced actin filament branching, resulting in long and infrequently branched actin filaments as opposed to the dendritic network formed by Arp2/3 alone (Blanchoin et al., 2001). Tropomyosin-decorated actin filaments are also protected from pointed end depolymerization and/or severing activity of ADF/cofilin (Bernstein and Bamburg, 1982; Broschat et al., 1989). Genetic experiments show that mutations in profilin suppress the bristle morphology phenotypes of capping protein (CP) mutants (Hopmann and Miller, 2003). For plant actin binding proteins, there is some biochemical data to show cooperativity, but virtually no genetic evidence. For example, Arabidopsis FIMBRIN1 (FIM1) stabilizes actin filaments against profilin-mediated depolymerization in vitro and in vivo (Kovar et al., 2000b). And both Arabidopsis CP (Huang et al., 2003) and poppy gelsolin (PrABP80; Huang et al., 2004) can prevent addition of the profilin–actin complex onto filament barbed ends. In this work, we show that VLN1-decorated actin filaments are protected from ADF activity in vitro, providing further evidence that actin binding protein activities and levels must be carefully orchestrated to generate and maintain particular actin structures in the plant cell.

Based on sequence similarity and conserved domain organization between villins from different kingdoms (e.g., 26% identity and 36% similarity between VLN1 and human villin), the plant villins have been assumed to maintain the full range of villin/gelsolin functions (Holdaway-Clarke and Hepler, 2003). We examined the properties of recombinant VLN1 by sedimentation, fluorescence light microscopy, and kinetic polymerization assays. We found that VLN1 binds with high affinity to F-actin and bundles actin filaments in a calcium- and calmodulin-insensitive manner. However, recombinant VLN1 does not sever, cap, and nucleate actin filament formation in vitro. This can be explained by the poor conservation of predicted type 1 and type 2 calcium binding sites in the gelsolin-like core of VLN1. During kinetic assays with ADF1, VLN1 appears to bind first and protects actin filaments from ADF-mediated depolymerization. Our findings support the conclusion that VLN1 efficiently promotes actin bundle formation and stabilizes it from actin depolymerizing factors.

RESULTS

Identification of a Calcium-Insensitive Villin Isoform

The Ca^{2+}-dependent activity of villin is contained in a core region, composed of six repeats, which displays strong homology to gelsolin (Glenney et al., 1981; Arpin et al., 1988; Bazari et al., 1988). The x-ray crystal structures of Ca^{2+}-free gelsolin and of the N- and C-terminal halves of gelsolin bound to actin have brought insight into the mechanism of Ca^{2+} activation of gelsolin (Burtnick et al., 1997, 2004; Robinson et al., 1999; Choe et al., 2002). The eight Ca^{2+} binding sites contained within gelsolin were predicted, through sequence homology, to also exist in human villin (Choe et al., 2002). Many of these sites have now been confirmed through mutagenesis studies (Kumar and Khurana, 2004; Kumar et al., 2004). We sought to determine whether these Ca^{2+} binding sites also exist in plant villins by aligning gelsolin, human villin, and plant villins based on the structural features determined for gelsolin, as shown in Figure 1.

The alignment shows that all plant villins contain the 4 amino acid signature of a gelsolin domain in 5 out of 6 of their gelsolin-homology domains (G1–G6; pink highlighting, Figure 1) with the exception, in each case, being domain G2 (Choe et al., 2002). Comparison of the residues that are involved in the tail latch, a structural feature that locks gelsolin in its inactive state, suggests that this feature will also be present in plant and human villins (red letters, Figure 1; Burtnick et al., 1997). Hence, the structures of inactive gelsolin and plant villins are likely to be similar. The villin tail latch precedes the headpiece domain, which in plants is separated by a variable length linker region (Vidali et al., 1999; Klahre et al., 2000). Comparison of the activated states of gelsolin and villins, judged by the conservation of residues that form the characteristic active interfaces between G2:G3 and G5:G6 (dark and light blue highlighting, respectively, Figure 1), suggests that plant villins may also be able to reach a similar final activated state to gelsolin. Furthermore, a general conservation of actin binding residues in plant villins indicates that the molecules will share many of the actin binding surfaces that have been determined for gelsolin (red highlighting, Figure 1).

Two classes of Ca^{2+} binding site have been identified: type 1 sites, where Ca^{2+} is bound at the interface between gelsolin and actin, mediating this interaction; and type 2 sites, where Ca^{2+} is bound exclusively by gelsolin and is responsible for activation (Choe et al., 2002). We compared the sequences of the plant villins with human gelsolin looking for differences in type 1 and type 2 sites (Figure 1). Type 1 Ca^{2+} binding sites (green highlighting, Figure 1) are present in G1 and absent from G4 in all the aligned plant villins. Furthermore, each G2 domain has a basic residue at its type 1 site, which has been proposed to mimic the calcium interaction (Choe et al., 2002). Type 2 sites (yellow highlighting, Figure 1) are present in each of the six gelsolin domains and in the six gelsolin-like domains of human villin. Arabidopsis VLN1 has the fewest type 2 sites, with only one site in G2 and a probable second site in G4, in which residue Glu475 is replaced by Asp. All other villins have at least three type 2 calcium binding sites. VLN2 and VLN3 and 135-ABP from lily pollen have the most, with four type 2 Ca^{2+}-sites in G1, G2, G4, and G6. All plant villins in this study have at least one domain where a basic residue replaces one of the acidic residues in the type 2 binding site, suggesting that these domains may achieve an active conformation and are not regulated by calcium. In summary, VLN1 has the fewest potential calcium binding sites, and hence is a strong candidate to be a Ca^{2+}-insensitive villin.

Purification of Recombinant VLN1

To analyze the functional properties of VLN1, the recombinant protein was expressed in *Escherichia coli* as a nonfusion construct from a T7 vector. A bacterial extract (Figure 2A, lane 1) was fractionated with ammonium sulfate precipitation (Figure 2A, lane 2), followed by chromatography on DEAE-Sephacel (Figure 2A, lane 3), Cibacron Blue 3G-A (Figure 2, lane 4), and Q-Sepharose (Figure 2A, lane 5). After elution from Q-Sepharose, the purity of VLN1 was >90% and typical yields were 5 mg from 1 liter of bacterial culture. The purified, recombinant protein cross-reacts with an affinity-purified antibody raised against the G1 to G3 domains of VLN1 (Figure 2B).

VLN1 Binds to F-Actin in a Calcium-Independent Manner

The ability of bacterially-expressed VLN1 to bind to F-actin was assayed with a high-speed cosedimentation assay, as shown in Figure 3. A majority of the polymerized actin (F-actin) sedimented at 200,000*g* (Figure 3A, lane 3). In the absence of F-actin, very little VLN1 or FIM1, a well-characterized, plant actin crosslinking protein (Kovar et al., 2000b), was sedimented (Figure 3A, lanes 9 and 15). However, a significant amount of VLN1 and FIM1 cosedimented in the presence of polymerized actin (Figure 3A, lanes 6 and 12). These results verified that VLN1 binds to F-actin.

To determine the affinity of VLN1 for binding to F-actin, increasing concentrations of VLN1 were incubated with preassembled F-actin as described previously for FIM1 (Kovar et al., 2000b). After sedimentation at 200,000*g*, the amount of bound and free VLN1 was quantified by densitometry. Figure 3B shows a representative experiment in which the concentration of bound VLN1 was plotted against the concentration of free VLN1. Similar results were obtained for FIM1 (Figure 3C). By fitting the representative experimental data with a hyperbolic function, K_d values of 0.99 μM for VLN1 and 0.67 μM for FIM1 were obtained. From three such experiments, mean K_d values (± SD) of 1.11 ± 0.27 μM ($n = 3$) for VLN1 and 0.56 ± 0.21 μM ($n = 3$) for FIM1 binding to F-actin were calculated. The latter result is consistent with the previously published value of 0.53 ± 0.18 μM for FIM1 (Kovar et al., 2000b). At saturation, the stoichiometry of VLN1:actin was 1:2.4.

To test for the ability of VLN1 to interact with plant actin filaments, identical experiments were performed with maize pollen actin (Ren et al., 1997). Apparent K_d values (± SD; $n = 3$) of 0.79 ± 0.19 μM and 0.97 ± 0.11 μM were determined for VLN1 binding to plant actin and rabbit actin, respectively. The binding was not statistically different (by paired *t* test) for interaction with two different sources of actin. For convenience, all subsequent experiments were performed with muscle actin.

We also tested whether the binding of VLN1 to F-actin was affected by Ca^{2+}. As shown in Figure 3D, 3 μM actin and 1 μM VLN1 were incubated under polymerizing conditions in the presence of 4.6 nM, 100 nM, 1.0 μM, 12 μM, or 1.0 mM free Ca^{2+}. The amount of VLN1 that cosedimented with F-actin was not appreciably different at any of these Ca^{2+} concentrations. The results confirmed that VLN1 binds to F-actin in a Ca^{2+}-insensitive manner.

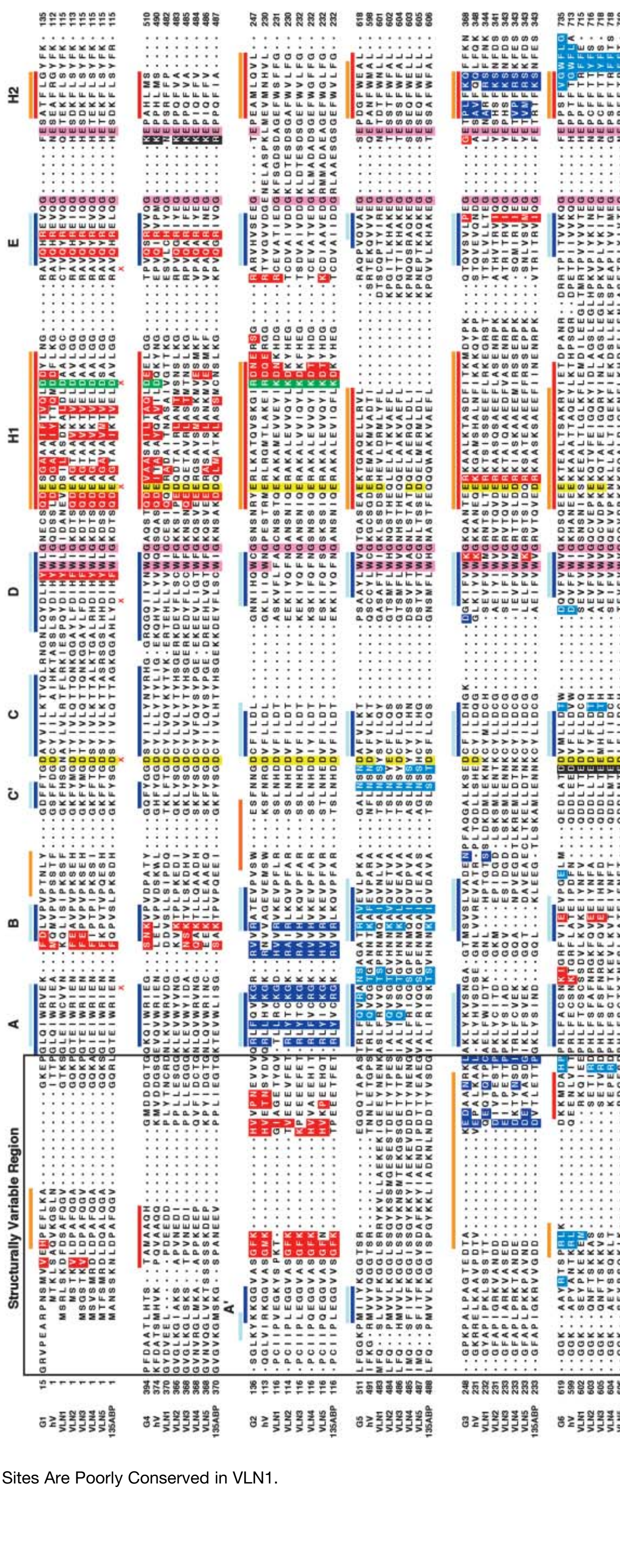

Figure 1. Ca^{2+} Binding Sites Are Poorly Conserved in VLN1.

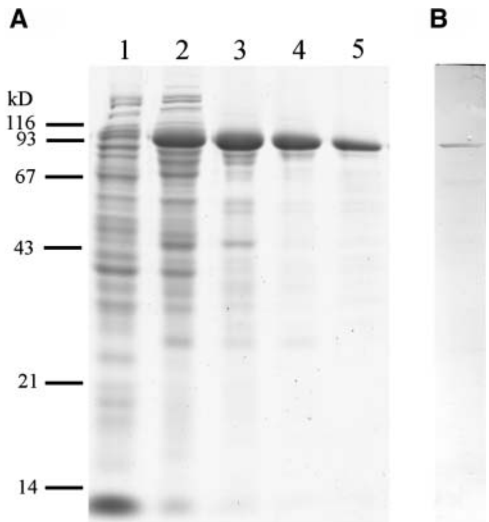

Figure 2. Purification of Recombinant VLN1.

(A) Coomassie Blue-stained protein gel of recombinant VLN1 purification. Lane 1, Total extract from bacterial cells (20 μg); lane 2, $(NH_4)_2SO_4$ precipitate (15 μg); lane 3, DEAE-Sephacel eluate (8 μg); lane 4, Cibacron Blue 3G-A eluate (4 μg); lane 5, Q-Sepharose eluate (2 μg). The migration of molecular mass (*MM*) standards is given at the left in kilodaltons.

(B) Protein immunoblot of purified VLN1 (100 ng) probed with affinity-purified, anti-VLN1(G1–G3) antibody.

VLN1 Bundles F-Actin in a Calcium-Insensitive Manner

The ability of VLN1 to bundle F-actin was examined with a low-speed cosedimentation assay. As shown in Figure 4, very little polymerized actin sedimented at 13,500*g* in the absence of actin binding protein (Figure 4A, lane 3). However, in the presence of VLN1, more polymerized actin sedimented (Figure 4A, lane 6), and the amount of the actin in the pellet increased in proportion to VLN1 concentration (data not shown).

Although the binding of VLN1 to actin filaments was not sensitive to Ca^{2+}, it was still of interest to determine whether the bundling activity was Ca^{2+}-dependent. We tested this by assaying the amount of bundled actin at different concentrations of Ca^{2+} (Figure 4B). Bundled actin was expressed as the amount of actin in the pellet determined by densitometry. When 3 μM actin and 1 μM VLN1 were polymerized in the presence of 4.6 nM, 100 nM, 1.0 μM, 12 μM, or 1.0 mM free Ca^{2+}, the percentage of actin in the pellet was 56.5, 60, 59.1, 55.9, and 63.9%, respectively. These results indicated that VLN1 bundles actin filaments in a Ca^{2+}-insensitive manner.

Lily pollen villins are regulated by Ca^{2+}-calmodulin (Ca/CaM). Specifically, the bundling activity of 135-ABP and 115-ABP is inhibited in the presence of 500 μM Ca^{2+} and 7 μM bovine CaM (Yokota et al., 2000, 2003). To test whether VLN1 might also be regulated in this fashion, we performed low speed sedimentation assays under conditions where 3 μM actin filaments and 200 nM VLN1 were allowed to interact in the presence of 500 μM free Ca^{2+} and varying amounts of CaM. As shown in Figure 4C (black bars), there was no difference in the amount of sedimentable actin filaments over two orders of magnitude (100 nM–10 μM) for [CaM]. Moreover, there was no detectable difference in the amount of VLN1 in the pellets (Figure 4C, gray bars). Similar results were obtained in the presence of 10 μM free Ca^{2+} (data not shown). These results demonstrate that VLN1 bundling activity was not inhibited by Ca/CaM.

A kinetic light scattering assay was used to monitor the dynamic process of VLN1 induced F-actin bundle formation. As shown in Figure 5A, light scattering was measured during the polymerization of 4-μM actin monomers (Figure 5A, dashed line) or after addition of varying amounts VLN1 (Figure 5A, closed symbols). The light scattering increased rapidly and almost reached steady state within 200 s, indicating that VLN1 binds to actin filaments quickly as they polymerize. When VLN1 concentration was raised from 0.2 to 0.5 μM, the final value of light scattering also increased, suggesting that more actin bundles were formed. One micromolar VLN1 was almost identical to 0.5 μM VLN1 (data not shown), suggesting that 0.5 μM VLN1 is sufficient to saturate the bundling sites of 4 μM F-actin. To confirm that the increase of light scattering during actin polymerization is mostly due to bundling and that villin has little effect on actin polymerization, we compared the variation of pyrene and light scattering during actin polymerization in the presence of 0.5 μM VLN1 (Figure 5B). Whereas VLN1 induced a large increase in light scattering during actin polymerization, it had little effect on the kinetics of polymerization as measured by pyrene fluorescence (Figure 5B, open squares = actin alone; open circles = actin and VLN1).

Figure 1. (continued).

A sequence alignment of plant villins based on the structural features determined for gelsolin. The six gelsolin domains are aligned against each other and labeled G1 to G6. These domains are ordered so that the most similar domains are paired (G1:G4, G2:G5, and G3:G6; Choe et al., 2002). GTAIL denotes the C-terminal extension, the tail latch. The boxed residues, labeled "Structurally Variable Region," do not show general structural homology between the six domains of gelsolin. Horizontal bars above the sequence show secondary structure and are labeled by letter according to the convention in Burtnick et al. (1997). Orange and red bars signify α-helices in the active and inactive states, respectively; similarly, light and dark blue bars represent β-strands in the active and inactive states (Burtnick et al., 1997, 2004; Choe et al., 2002). Human villin (hV; accession no. NP_009058), the five Arabidopsis villins (VLN1–5; NP_029567, NP_565958, NP_567048, AAO64915, NP_200542), and 135-ABP (AAD54660) are aligned against the gelsolin domains. Structural homology is represented as follows: the gelsolin domain signature residues are highlighted in pink; residues that form the active state, domain-domain interactions between G2:G3, G5:G6, and G4:G6 are colored dark blue, light blue, and gray, respectively; tail-latch residues that interact with G2, in the inactive conformation, are shown in red type; residues that interact with actin are depicted with red highlighting; type 1 and type 2 calcium ion coordinating residues are shown with green and yellow highlighting, respectively. Red Xs denote residues implicated in Ca^{2+} regulation by mutagenesis of vertebrate villin (Kumar et al., 2004).

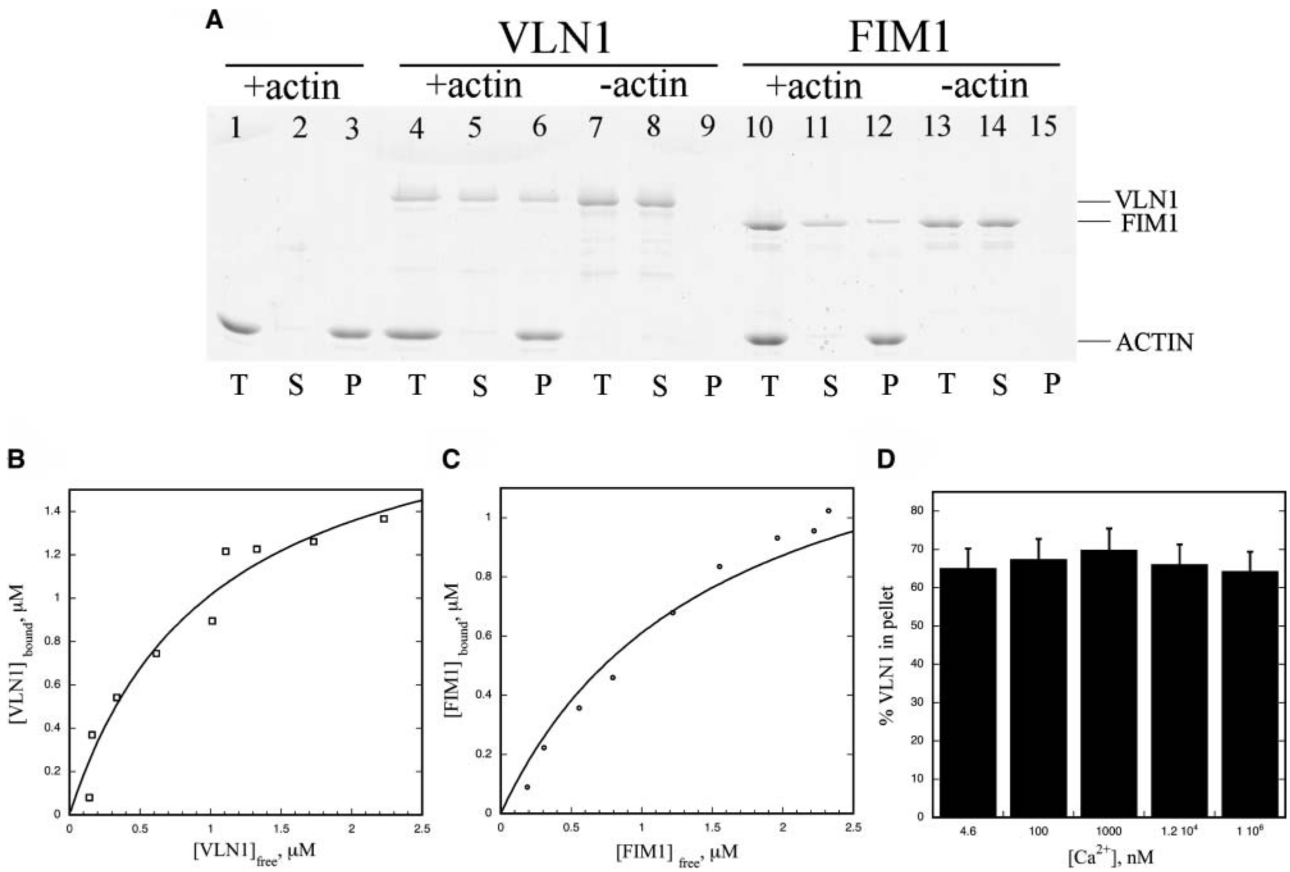

Figure 3. VLN1 Binds to F-Actin in a Calcium-Independent Manner.

(A) A high-speed cosedimentation assay was used to determine VLN1 binding to F-actin. A mixture of 3 μM F-actin and 1 μM VLN1, or 3 μM F-actin and 1 μM FIM1, was centrifuged at 200,000*g* for 1 h. The resulting supernatants and pellets were subjected to SDS-PAGE and Coomassie-stained. The position of actin, VLN1, and FIM1 are marked at the right. The samples include: lane 1, actin alone total; lane 2, actin alone supernatant; lane 3, actin alone pellet; lane 4, actin plus VLN1 total; lane 5, actin plus VLN1 supernatant; lane 6, actin plus VLN1 pellet; lane 7, VLN1 alone total; lane 8, VLN1 alone supernatant; lane 9, VLN1 alone pellet; lane 10, actin plus FIM1 total; lane 11, actin plus FIM1 supernatant; lane 12, actin plus FIM1 pellet; lane 13, FIM1 alone total; lane 14, FIM1 alone supernatant; lane 15, FIM1 alone pellet.

(B) Increasing concentrations of VLN1 (0.3–3.4 μM) were cosedimented with 3 μM F-actin. The concentration of bound VLN1 was plotted against the concentration of free VLN1 and fitted with a hyperbolic function. For this representative experiment, the calculated dissociation constant (K_d) was 0.99 μM.

(C) Identical experiments to that shown in **(B)** were performed with FIM1. For this representative experiment, the K_d value was 0.67 μM.

(D) Experiments similar to those described for **(A)** were repeated ($n = 3$) and extended to include different free [Ca^{2+}]. The resulting gels were scanned to determine the amount of VLN1 that was present in the pellet fraction under each condition. The percentage of VLN1 that cosedimented with F-actin at 4.6 nM Ca^{2+} was 65.0; at 100 nM Ca^{2+} was 67.4; at 1 μM Ca^{2+} was 69.9, at 12 μM Ca^{2+} was 66.1; and at 1 mM Ca^{2+} was 64.2.

Fluorescence light microscopy was used to visualize the effect of VLN1 on actin filaments. When 4 μM actin was polymerized in the presence of an equimolar amount of rhodamine-phalloidin and diluted to a final concentration of 10 nM before attaching to polylysine-coated cover slips, only individual actin filaments were detected in the field (Figure 5C). By contrast, when actin was polymerized in the presence of 0.5 μM VLN1 (Figure 5D) long actin filament bundles were detected. If we increased the concentration of VLN1, more higher-order actin bundles formed and the number of individual actin filaments decreased (data not shown).

VLN1 Does Not Nucleate, Cap, or Sever Actin Filaments

Vertebrate villin and gelsolin have nucleation, barbed end capping, and severing activities under certain calcium conditions (Friederich et al., 1999). However, plant villins (e.g., 135-ABP or 115-ABP from lily) have not been shown to have any of these activities (Yokota and Shimmen, 1999, 2000; Yokota et al., 2003) perhaps because of the limited numbers of ways that interactions with F-actin have been tested. We therefore tested this possibility by nucleation, elongation, and depolymerization assays previously established for the analysis of Arabidopsis AtCP (Huang et al., 2003) and poppy gelsolin (PrABP80; Huang et al., 2004).

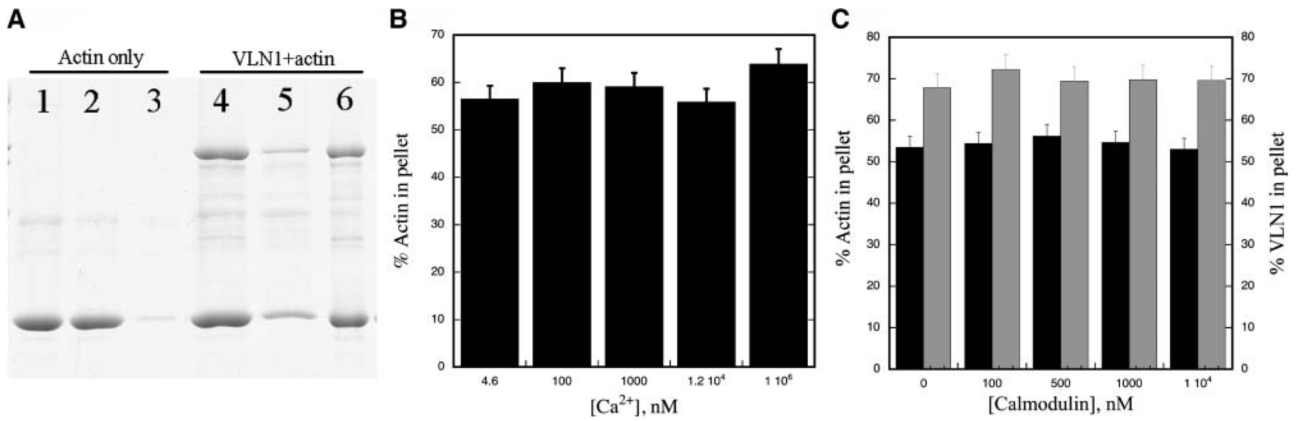

Figure 4. VLN1 Bundles F-Actin in a Calcium- and Calmodulin-Independent Manner.

(A) A low-speed cosedimentation assay was used to determine the bundling activity of VLN1. Actin alone (3 μM) and actin plus 1 μM VLN1 were incubated under polymerization conditions and the reactions were centrifuged at 13,500*g*. Equivalent amounts of total, supernatant, and pellet were separated by SDS-PAGE. Samples are: lane 1, actin alone total; lane 2, actin alone supernatant; lane 3, actin alone pellet; lane 4, actin plus VLN1 total; lane 5, actin plus VLN1 supernatant; and lane 6, actin plus VLN1 pellet.

(B) To determine whether calcium affects bundling activity, the experiments described in **(A)** were repeated ($n = 3$) in the presence of varying free Ca^{2+} concentrations. The resulting gels were scanned to determine the amount of actin in the pellet at different free [Ca^{2+}]. The percentage of actin sedimenting at 4.6 nM Ca^{2+} was 56.5%; at 100 nM Ca^{2+} was 60%; at 1 μM Ca^{2+} was 59.1; at 12 μM Ca^{2+} was 55.90; and at 1 mM Ca^{2+} was 63.9%.

(C) To test the effects of calmodulin, 3 μM actin and 200 nM VLN1 were incubated in the presence of 500 μM free [Ca^{2+}] and various amounts of calmodulin. The resulting gels were scanned to determine the percentage of actin (black bars) and VLN1 (gray bars) that sedimented under each condition.

Experiments to examine the effect of VLN1 on the dynamics of actin polymerization from monomers were performed. As shown in Figure 6A, when pyrene fluorescence was used to monitor rabbit muscle actin polymerization kinetically, the initial lag corresponding to the nucleation step decreased with increasing human plasma gelsolin (GS) concentration. However, in the presence of various concentrations of VLN1, the initial actin polymerization rate did not change compared with actin alone (Figure 6A). These results indicate that VLN1 does not have nucleation activity.

Seeded elongation assays were performed to address whether VLN1 has capping activity. The elongation rate depends on the availability of actin filament barbed ends, under these experimental conditions: 0.4 μM preformed F-actin was incubated with varying concentrations of VLN1 or GS for 5 min and polymerization initiated with addition of 1 μM G-actin (5% pyrene labeled) at a free [Ca^{2+}] of 1 μM. The G-actin was saturated with 4 μM human profilin to prevent spontaneous nucleation and elongation from pointed ends (Pollard and Cooper, 1984). The results showed that the initial elongation rate was decreased with various amounts of GS (Figure 6B). However, no change of initial elongation rate was observed in the presence of different concentrations of VLN1. These results indicate that VLN1 does not have barbed-end capping activity.

The influence of VLN1 and GS on actin filament depolymerization was investigated by adding equimolar amounts of profilin (2.5 μM) to pyrene-labeled F-actin and monitoring the decrease in fluorescence. The results from a typical experiment in the presence of 10 μM free Ca^{2+} are shown in Figure 6C. The depolymerization rate was increased by adding various amounts of GS, compared with actin alone. By comparison, VLN1 did not increase the depolymerization rate, indicating that VLN1 does not have severing activity.

VLN1 Stabilizes Actin Filaments and Protects Them from ADF-Mediated Depolymerization

Microinjection of antiserum against 135-ABP into living root hair cells induced the disappearance of transvacuolar strands (Tominaga et al., 2000; Ketelaar et al., 2002), suggesting that plant villin stabilized actin filaments in vivo and protected them from depolymerization. Plant ADF has been shown to be a potent depolymerizing factor in vitro (Lopez et al., 1996; Carlier et al., 1997; Maciver and Hussey, 2002). To test whether VLN1 can stabilize actin filaments against ADF-induced depolymerization, pyrene-labeled actin filaments were incubated with VLN1 before addition of ADF1 and latrunculin B. In these experiments, latrunculin is used to synergize with ADF during actin depolymerization by preventing readdition of actin subunits to filament barbed ends. The rapid decrease in fluorescence after addition of ADF1 and latrunculin B to pyrene labeled actin filaments is mainly due to binding of ADF1 to actin filaments (Figure 7A, open triangles; Carlier et al., 1997), whereas the slow decrease in pyrene fluorescence is due to actin filament depolymerization (Figure 7A, open triangles). Addition of ADF1 to pyrene-labeled-actin filaments preincubated with VLN1 induced only a small change in pyrene fluorescence (Figure 7A, open diamonds), suggesting that actin filaments incubated with VLN1 before addition of ADF1 are protected against binding and subsequent depolymerization induced by ADF1.

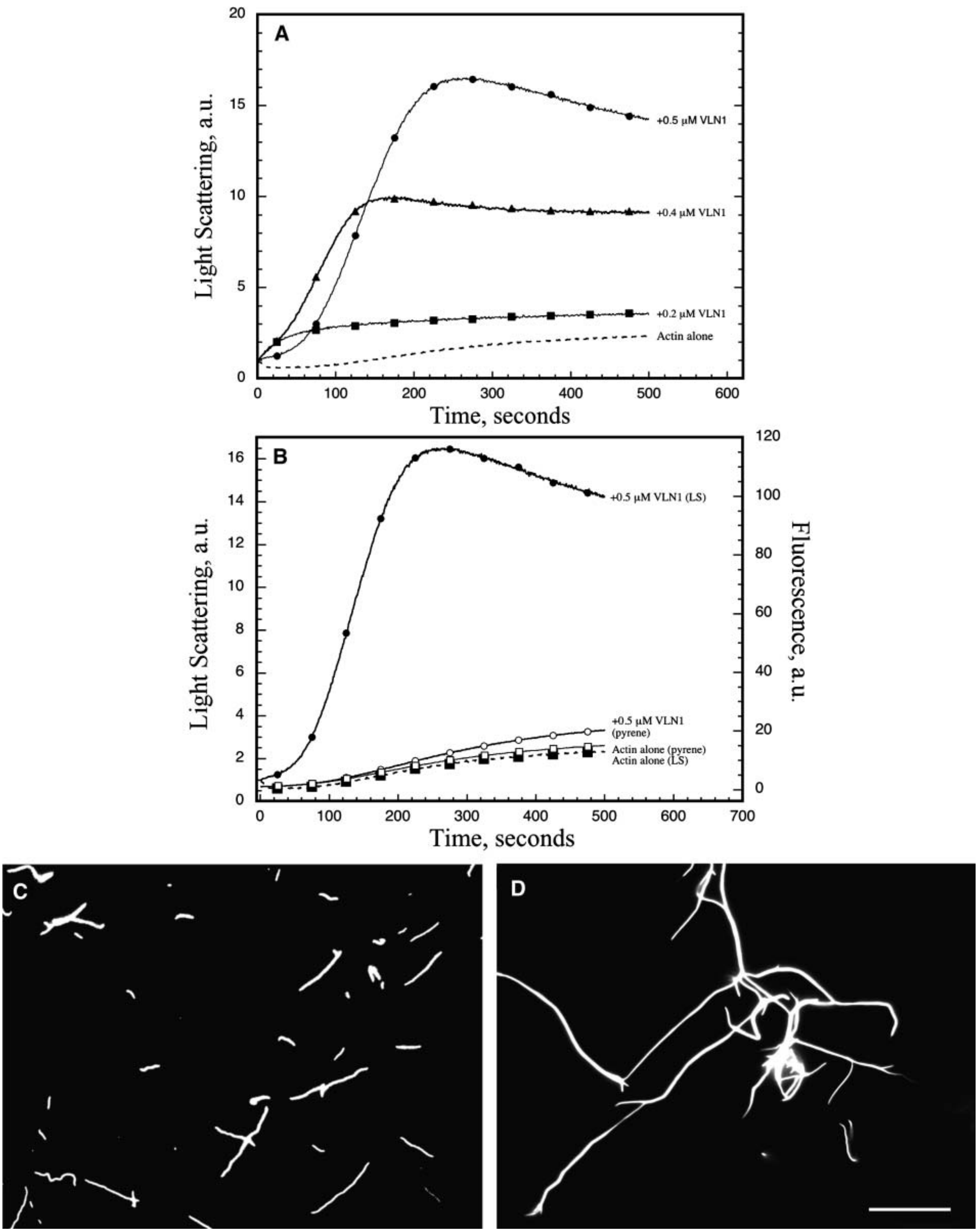

Figure 5. Villin Rapidly Bundles Actin Filaments But Does Not Affect the Rate of Actin Polymerization.

Conditions: 4 μM actin, 10 mM Tris-HCl, pH 7, 50 mM KCl, 2 mM $MgCl_2$, 1 mM EGTA, 0.2 mM ATP, 0.2 mM $CaCl_2$, 0.5 mM DTT, and 3 mM NaN_3 at 20°C.
(A) Time course of polymerization monitored by light scattering. Dashed line, no additions to actin; filled squares, addition of 0.2 μM villin; filled triangles, addition of 0.4 μM villin; filled circles, addition of 0.5 μM villin.

A spontaneous polymerization assay established that VLN1 protects elongated actin filaments against ADF (Figure 7B). After a lag corresponding to the nucleation step, ADF1 increased the rate of polymerization by generating a higher concentration of filament barbed ends (Figure 7B, closed squares) than the control without ADF1 (Figure 7B, dashed line). Addition of VLN1 in the polymerization mixture inhibited the effect of ADF (Figure 7B, open squares). These results suggested that VLN1 binds rapidly to elongated actin filaments and prevents further binding of ADF to actin filaments.

Fluorescence light microscopy was used to visualize the effect of both ADF1 and VLN1 on actin filaments, as shown in Figure 8. Actin filaments polymerized in the presence of 3 μM ADF1 had a much shorter mean length (Figure 8C; 2.5 μm) than actin alone (Figure 8A; 12 μm). By contrast, when actin was polymerized in the presence of 0.5 μM VLN1 (Figure 8B) long actin filament bundles were detected. In the presence of both VLN1 and ADF1 similar long actin filaments bundles were observed (Figure 8D), suggesting that bundles generated by VLN1 are resistant to ADF-induced severing and depolymerization.

DISCUSSION

Here, we describe the biochemical characterization of VLN1 and its possible implication in actin cable formation and stabilization. The Arabidopsis VILLIN family (AtVLN) contains five isoforms encoded by *VLN1−5*. Each predicted AtVLN protein is composed of a core with six gelsolin homology domains followed by the C-terminal villin headpiece. Recombinant VLN1 binds to actin filaments and generates bundles in vitro. Surprisingly, VLN1 did not nucleate, cap, or sever actin filaments. VLN1 is the first villin/gelsolin family member from the plant kingdom that is not Ca^{2+} regulated, nor is its activity modulated by CaM like several other plant villins. During actin polymerization, bundles of actin filaments are generated rapidly by VLN1 and are resistant to depolymerization induced by ADF1, suggesting a potential mechanism for actin cable formation and stabilization in vivo. Neither the affinity for binding to actin filaments nor the bundling efficiency are affected by the source of actin (i.e., maize pollen or rabbit skeletal muscle).

Cosedimentation assays provide additional insight about the binding of VLN1 to actin filaments and the bundling activity of VLN1. VLN1 binds actin filaments with an apparent K_d of 1 μM. The recombinant V2–V3 and headpiece domains from chicken villin have reported K_d values of 0.3 and 7 μM, respectively (Pope et al., 1994). Drosophilia Quail, a villin-related protein, binds actin filaments with a stronger affinity (7 nM; Matova et al., 1999). Low speed cosedimentation assays show that VLN1 is an efficient bundler with a maximum effect at a ratio of 1:6 villin to actin (data not shown). Both the affinity of VLN1 for actin filaments and the bundling activity were independent of free Ca^{2+} concentrations ranging from 4.6 nM to 1 mM. Moreover, and distinct from the lily pollen villins 135-ABP and 115-ABP (Yokota et al., 2000, 2003), bundling was unaffected by up to 500 μM free Ca^{2+} and 10 μM CaM. The effect of VLN1 on actin assembly was characterized with a combination of light scattering, pyrene fluorescence, and light microscopy. An increase in light scattering can reflect both an increase in the amount of polymerized actin and a bundling effect, whereas pyrene fluorescence is not affected by bundling and reflects only an increase in the amount of polymerized actin. During actin polymerization, the presence of VLN1 induces a large increase of light scattering but no change in pyrene fluorescence, suggesting that VLN1 is only an actin filament bundling protein. Direct visualization of actin filaments by light microscopy confirmed the bundling activity of VLN1. The presence of VLN1 in the polymerization mixture transforms individual actin filaments into large actin filament bundles of more than 50 μm in length. Together with the fact that VLN1 has no effect in the seeded elongation assay or on filament depolymerization, our data are consistent with VLN1 being a simple actin filament bundling protein that is not regulated by Ca^{2+}/CaM.

Multiple Ca^{2+} binding sites have been identified in villin (Hesterberg and Weber, 1983). The Ca^{2+} binding sites in the core region (gelsolin homology domains) are responsible for the Ca^{2+}-dependent activation of villin, whereas Ca^{2+} binding in the headpiece domain is not involved in any calcium regulated function of villin (Glenney and Weber, 1981; Arpin et al., 1988; Bazari et al., 1988; Kumar and Khurana, 2004). Based on the high sequence homology between the core domains of gelsolin and villin it is fair to propose that the mechanism of Ca^{2+}-dependent activation for gelsolin and villin will be similar. Indeed, the NMR structure of human villin shows conserved residues with gelsolin in type 1 Ca^{2+} binding sites (Markus et al., 1997; Choe et al., 2002). Sequence alignment predicted that VLN1 would have a minimal Ca^{2+}-dependent activation (Figure 1). Compared with other plant villins, VLN1 has the fewest potential Ca^{2+} binding sites with only one type 2 site in G2 and a potential second site in G4. Lily pollen 135-ABP (Vidali et al., 1999), VLN2, and VLN3 have the most, with four type 2 Ca^{2+}-sites in G1, G2, G4, and G6, suggesting that some of the core activities of these villins will be relatively more Ca^{2+}-sensitive. Dissection of Ca^{2+}-sensitive sites involved in the control of capping and depolymerization induced by human villin identified two functional types of Ca^{2+}-sensitive sites. The G1 type 1 and 2 sites (Glu25, Asp44, Glu74; and Asp86,

Figure 5. (continued).

(B) Comparison of actin polymerization monitored by pyrene fluorescence and light scattering. Filled squares, polymerization of actin alone monitored by light scattering; filled circles, polymerization of actin in presence of 0.5 μM villin monitored by light scattering; open squares, polymerization of actin alone monitored by pyrene fluorescence; open circles, polymerization of actin in presence of 0.5 μM villin monitored by pyrene fluorescence.

(C) and **(D)** Micrograph of actin bundles in the presence of VLN1 in vitro. The ability of VLN1 to form actin bundles was visualized by fluorescence light microscope with rhodamine-phalloidin staining. Scale bar = 10 μm.

(C) Individual actin filaments formed in the absence of VLN1.

(D) Bundles of actin filaments in the presence of 500 nM VLN1.

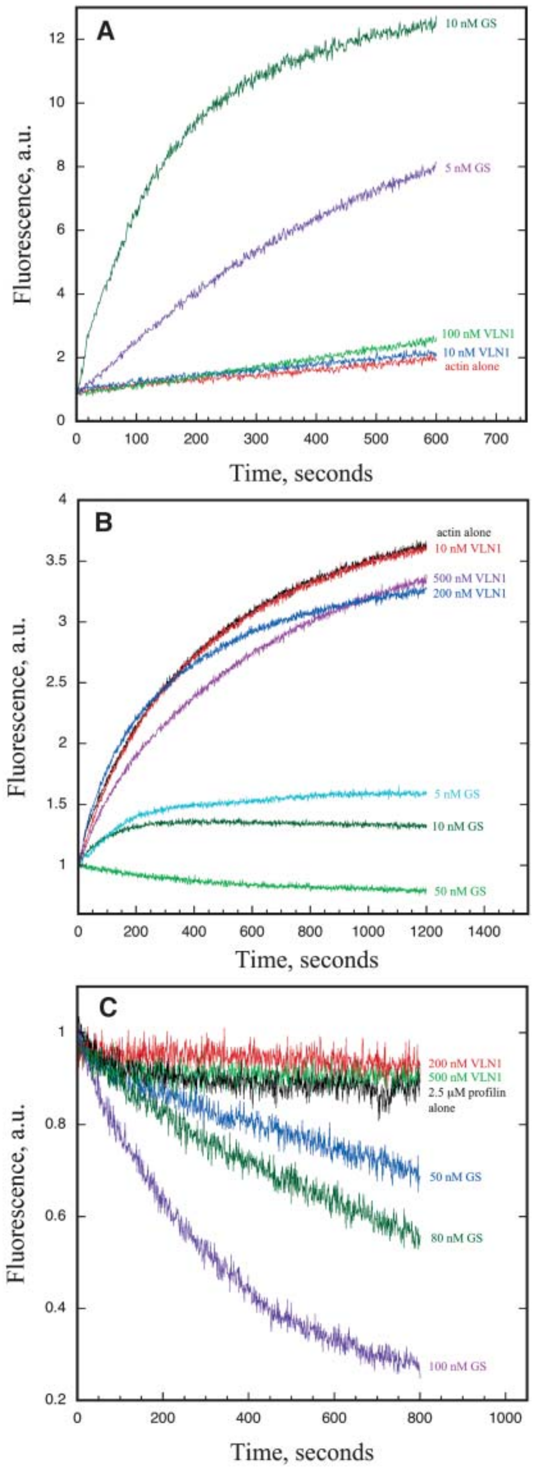

Figure 6. VLN1 Does Not Have Nucleation, Capping, or Severing Activity.

(A) VLN1 lacks nucleation activity. VLN1 or GS at the concentrations noted on the figure were incubated for 5 min with 2 μM actin (5% pyrene-labeled) before polymerization. Pyrene fluorescence was plotted versus time after addition of polymerization buffer.

(B) VLN1 lacks capping activity. Preformed F-actin (0.4 μM) seeds were incubated with different concentrations of VLN1 and GS, as noted on the figure. One micromolar G-actin saturated with 4 μM human profilin I was added to initiate actin elongation at the barbed end. The change in pyrene-actin fluorescence accompanying polymerization was plotted versus time after addition of G-actin.

(C) VLN1 lacks severing activity. *Zea mays* profilin (ZmPRO5; 2.5 μM) alone or ZmPRO5 together with VLN1 or GS were added to a F-actin solution prepared from 2.5 μM actin (40–50% pyrene-labeled). Depolymerization was recorded by reduction in pyrene fluorescence beginning from the addition of protein. All reactions are performed in the presence of 10 μM free Ca^{2+}.

Ala93, Asp61, respectively; red crosses, Figure 1) control actin depolymerization, whereas the G1 type 2 site alone is responsible for regulation of actin capping (Burtnick et al., 2004; Kumar et al., 2004). Glu25, Asp44, and Ala93 are conserved in all plant villins except VLN1. Moreover, mutation of Ala93 by another uncharged amino acid (Gly) inhibits the conformational changes induced by Ca^{2+} in the G1 domain of human villin (Kumar and Khurana, 2004). In VLN1, Ala93 is replaced by Thr, a polar uncharged amino acid, providing a potential explanation for the lack of Ca^{2+}-sensitive depolymerization activity in VLN1. The Ca^{2+}-insensitive villin-related protein QUAIL has one type 2 site in G5 and one type 1 site in G1. QUAIL is missing eight residues from the G1-G2 linker; hence, this protein cannot reach from the capping site of G1 to the filament binding site of G2 (Burtnick et al., 2004), meaning that it will not be able to sever. However, the plant villins appear to have a conserved tail latch (Figure 1). Despite the lack of Ca^{2+} activation for VLN1, this protein is able to crosslink filaments, which suggests that the tail latch is released by another mechanism. A possible mechanism would be that actin filament binding by the villin headpiece releases the tail latch from G2, exposing the filament binding surface of G2 and allowing interaction with a second filament.

The biochemical analysis determined that VLN1 not only is insensitive to calcium but also lacks the actin capping/severing functionality of human gelsolin and villin. A more detailed look at the conservation of the actin binding residues in VLN1 shows that many of these residues are absent from the capping domains (G1 and G4; red and green highlighting, Figure 1). Furthermore, actin binding residues in the structural variable region of G2 are also absent. This region snakes across the surface of actin linking the capping domain, G1, to the side binding domain, G2 (Burtnick et al., 2004). In contrast with the actin binding site of G2, the F-actin binding domain appears to be present (residues 199–206; red and green highlighting, Figure 1). Taken together, VLN1 shows sequence variation with respect to human gelsolin and villin that is consistent with its loss of capping and severing functionalities and with its inability to respond to calcium.

In plant cells, actin filaments are often organized in long actin cables (or bundles); these structures are used as tracks for cytoplasmic streaming, which is essential for transporting material required for cell elongation (Shimmen and Yokota, 2004). During pollen tube growth, an example of tip growth, there is remarkable coordination between cell expansion, Ca^{2+} oscillations, and actin polymerization/depolymerization. Increases in cytosolic free calcium ($[Ca^{2+}]_i$) are correlated with a decrease in

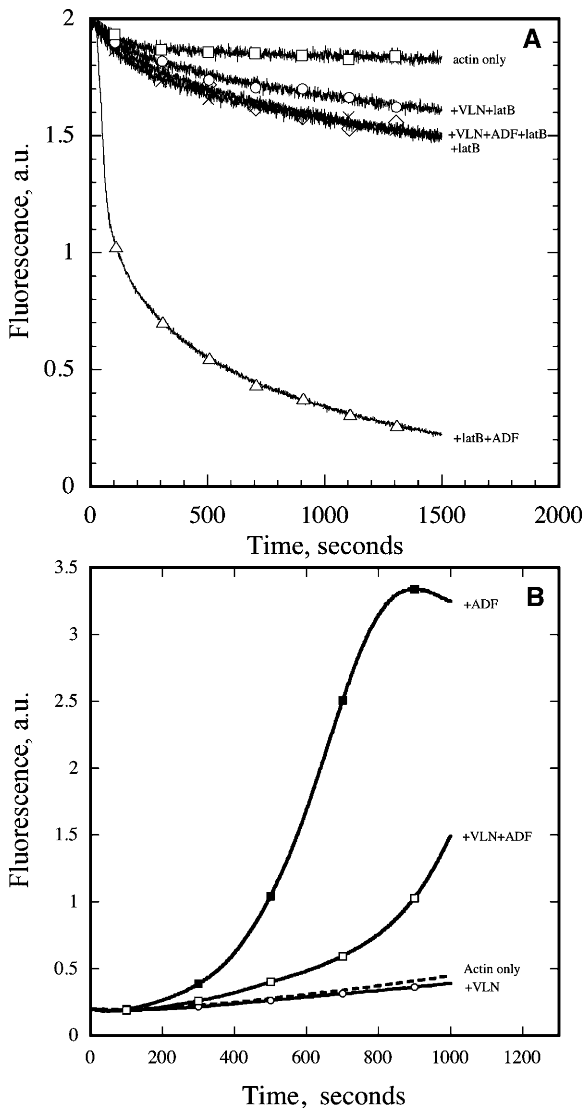

Figure 7. VLN1 Stabilizes Actin Filaments against ADF.

Conditions: 10 mM Tris-HCl, pH 8, 50 mM KCl, 2 mM $MgCl_2$, 1 mM EGTA, 0.2 mM ATP; 0.2 mM $CaCl_2$, 0.5 mM DTT, and 3 mM NaN_3 at 20°C.

(A) Time course of actin filament depolymerization monitored by pyrene fluorescence. Open squares, 1 μM actin filaments alone; open diamonds, 1 μM F-actin with 8 μM latrunculin B (LatB); open circles, 1 μM F-actin with 8 μM LatB and 1 μM VLN1; crosses, 1 μM F-actin with 0.6 μM ADF1, 8 μM LatB and 1 μM VLN1; and open triangles, 1 μM F-actin with 0.6 μM ADF1 and 8 μM LatB.

(B) Time course of actin polymerization (4 μM) monitored by pyrene fluorescence. Dashed line with no symbols, no additions to actin; open circles, actin with 1 μM VLN1; closed squares, actin with 1 μM ADF1; and open squares, actin with 1 μM VLN1 and 1 μM ADF1.

actin filaments near the tip, but actin cables present all along the pollen tube seem resistant to these $[Ca^{2+}]_i$ changes (Fu et al., 2001). The presence of actin bundles generated by VLN1 will protect these actin filaments against depolymerization induced by $[Ca^{2+}]_i$ oscillations. 115-ABP and 135-ABP colocalize with long actin cables (or bundles) in lily pollen, but these two villins are Ca^{2+}/CaM-sensitive (Yokota et al., 2000, 2003). An increase in $[Ca^{2+}]_i$ should induce actin filament fragmentation and further depolymerization of actin cables by both lily villins (Yokota and Shimmen, 2000), similar to the reorganization of actin filaments observed at the apex of the pollen tube. Identification of gelsolin from *Papaver rhoeas* pollen (Huang et al., 2004) and fragmin from *L. davidii* pollen (Fan et al., 2004) provide alternative mechanisms used by plants to regulate Ca^{2+}-mediated fragmentation and depolymerization of actin filaments. GeneChip data indicate that VLN1 and VLN2 are indeed expressed in Arabidopsis pollen, but neither isoform is very abundant (C. Pina, J. Becker, and J. Feijó, personal communication). By comparison, VLN5, which is predicted to be a Ca^{2+}-regulated severing and capping protein, is highly abundant in pollen. VLN5 and VLN2, with three or four conserved type-1 Ca^{2+} binding sites, respectively (Figure 1), are likely to be the major villin/gelsolin isoforms that respond to Ca^{2+} fluxes in the pollen tube apical region, whereas VLN1 may stabilize the axial actin cables. More work is clearly needed to understand how the different isoforms of villin and gelsolin are coordinated to generate actin cables that are Ca^{2+}-sensitive or -insensitive depending on their in vivo functions and subcellular distribution.

The presence of VLN1, a Ca^{2+}-insensitive villin/gelsolin family member, may reflect an adaptation of plants to separate Ca^{2+}-signaling and direct control of actin dynamics to maintain the stability of the actin cables. Klahre et al. (2000) show that VLN1, although less abundant than other isoforms, is expressed in all tissues examined by RNA gel blot analysis. Promoter-GUS fusions demonstrate high levels of VLN1 in root and leaf vascular tissue, root tips, guard cells, and trichomes (Klahre et al., 2000). A query of current microarray databases using the GENEVESTIGATOR program (www.genevestigator.ethz.ch; Zimmermann et al., 2004) confirms that VLN1 is widely expressed during the development of Arabidopsis plants, but may be upregulated during bolting. Tissue microarray data indicate an abundance of VLN1 transcript in hypocotyls and the shoot apex, but diminished levels in senescing leaves, adult and cauline leaves, sepals, and cotyledons. Moreover, VLN1 is upregulated in response to several types of stress, including temperature and osmotic stress, as well as infection with *Agrobacterium tumefaciens*. This seems significant because many biotic and abiotic stresses stimulate transient changes in cytosolic Ca^{2+} and rearrangements of the cytoskeleton (Staiger, 2000; Drøbak et al., 2004). Localization data with isoform-specific antibodies, or full-length VILLIN–GFP fusion proteins, will provide further information about where within the plant the different isoforms are distributed and whether they associate with specific actin arrays at the subcellular level. Finally, reverse-genetic analyses can be used to dissect a role for VILLIN in stabilization of actin filaments and generation of bundled arrays. In particular, insertional mutants will facilitate analyses of functional redundancy between VILLIN isoforms, as well as between VILLIN and

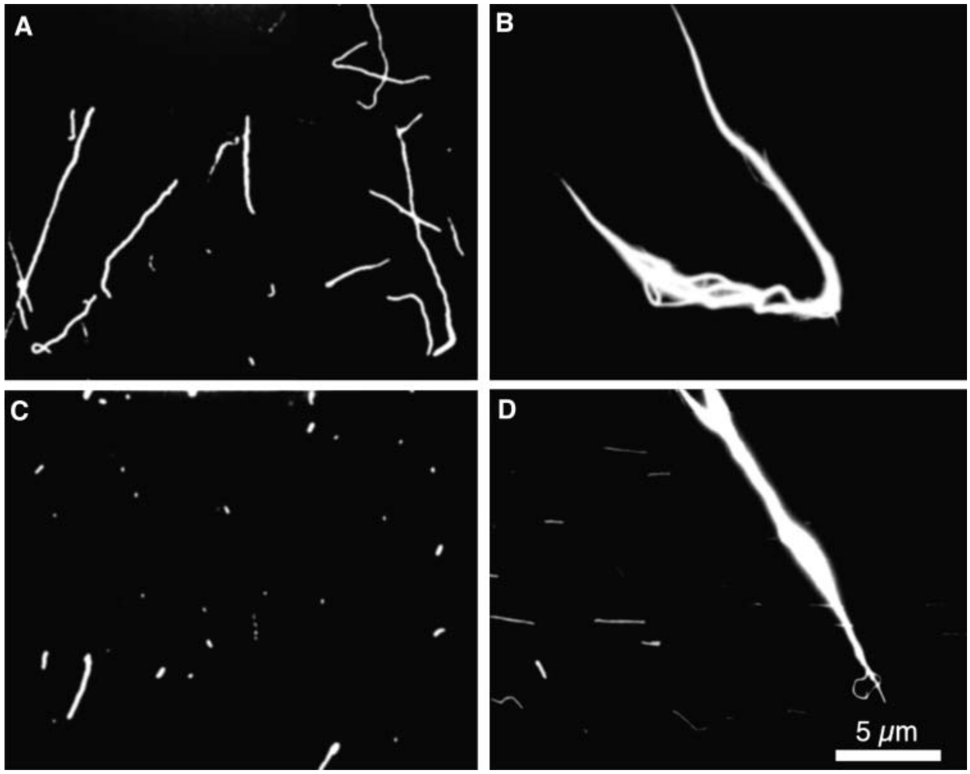

Figure 8. Micrograph of Actin Filaments in the Presence of VLN1 and ADF.

The ability of VLN1 to form stable actin bundles in the presence of ADF was visualized by fluorescence light microscope with rhodamine-phalloidin staining. The scale bar in **(D)** represents 5 μm.
(A) Actin filaments formed in the absence of VLN1.
(B) Actin filaments in the presence of 1 μM VLN1.
(C) Actin filaments in the presence of 3 μM ADF.
(D) Actin filaments in the presence of 3 μM ADF and 1 μM VLN1.

FIMBRIN. If VLN1 function is partially redundant, we predict that the protein with overlapping function and expression pattern is Arabidopsis FIMBRIN2. This actin bundling protein has nearly identical biochemical properties, including Ca^{2+}-independent filament bundling activity and the ability to stabilize filaments against dilution- and profilin-mediated depolymerization, as well as a similar expression pattern in the plant (L.Y. Gao, D.W. McCurdy, and C.J. Staiger, unpublished data).

In addition to Ca^{2+}-induced actin depolymerization, a major actin depolymerizing factor in plants is ADF/cofilin (Lopez et al., 1996; Carlier et al., 1997; Ressad et al., 1998; Dong et al., 2001; Smertenko et al., 2001; Chen et al., 2002; Hussey et al., 2002; Maciver and Hussey, 2002). After actin polymerization, ATP hydrolysis and phosphate release control ADF/cofilin binding and depolymerization of actin filaments (Maciver et al., 1991; Blanchoin and Pollard, 1999). As ADF/cofilin increases the rate of phosphate release from actin filaments (Blanchoin and Pollard, 1999), depolymerization will occur rapidly ($t_{1/2} < 30$ s; Pollard et al., 2000). Long-lived actin cables (or bundles) have to be protected against ADF-induced actin depolymerization (Pollard et al., 2000). Preformed bundles of actin filaments generated by VLN1 are protected against depolymerization induced by ADF1, suggesting a similar effect between VLN1 and tropomyosin, which inhibits ADF/cofilin binding and depolymerization (Bernstein and Bamburg, 1982; Nishida et al., 1985). Pope et al. (1994) showed that the villin headpiece competes with human ADF for binding to actin filaments but did not demonstrate a protection against depolymerization. Which region of VLN1 stabilizes filaments, whether it is the gelsolin-like core, the headpiece, or both, has not been determined. During active polymerization, the situation is more complex because to protect actin filaments against ADF/cofilin, VLN1 has to bind first to actin filaments and rapidly bundle them. We found that as actin filaments elongate VLN1 indeed binds before any appreciable binding of ADF/cofilin. A possible explanation is that the binding of ADF/cofilin to actin filaments is delayed by ATP hydrolysis and phosphate release from the filament, whereas the binding of villin to actin filaments is independent of the nucleotide state of actin filaments. In agreement with this data, a moderate amount of GFP-NtADF expressed in pollen tubes is localized with actin filaments of the fringe region near the apex and not with actin filament cables deeper in the pollen tube (Chen et al., 2002).

The Arabidopsis villin family contains multiple isoforms of actin binding proteins that are likely to play central roles in regulating actin filament dynamics and the formation of higher-order actin arrays. Understanding the function of the actin cytoskeleton requires detailed knowledge of how different classes of actin binding protein work in concert or in competition to construct or dismantle populations of filaments. VLN1 is the first plant villin to be described with a function that is independent of [Ca^{2+}]. Its biochemical properties are consistent with a role in creating and/or stabilizing actin filament bundles, such as those found in pollen tubes and root hairs or in the transvacuolar cytoplasmic strands of highly vacuolate cells. Villin was originally discovered as the major actin binding protein of the intestinal microvillus (Bretscher and Weber, 1979, 1980). Perhaps similar to plant cells, microvilli lack tropomyosin and have a population of stable actin filaments (Heintzelman and Mooseker, 1992). Our findings provide insight to why villin-containing actin filament bundles in microvilli are stabilized against the major actin depolymerizing factor (ADF/cofilin).

METHODS

Protein Production

A full-length cDNA for *Arabidopsis thaliana VLN1* was isolated from a size-fractionated root cDNA library (CD4-16; Arabidopsis Biological Resource Center, Ohio State University) using the EST H5D9 (*Hin*dIII fragment) as a probe. The clone was sequenced and confirmed to match exactly a cDNA with accession number AF081201 present in GenBank (Klahre et al., 2000). The coding sequence for VLN1 was amplified by PCR, subcloned into pET23a, and confirmed by sequencing. The VLN1-pET23a construct was transformed into *Escherichia coli* BL21 (DE3) cells and grown overnight at 37°C. After subculturing into fresh media, cells were grown at 37°C for 2 h, then induced for 8 h at 15°C with the addition of 0.4 mM isopropyl β-D-thiogalactopyranoside. Cells were collected by centrifugation and resuspended in 50 mM Tris-HCl, pH 8.0, supplemented with a 1:200 dilution of protease inhibitors from a stock solution (Ren et al., 1997), and sonicated. The sonicate was clarified at 46,000*g*. The VLN1 protein was precipitated from the supernatant with $(NH_4)_2SO_4$ at 45% saturation. The pellet was dissolved in Solution A containing 10 mM KCl, 1 mM DTT, and 10 mM Tris-HCl, pH 7.0, supplemented with a 1:200 dilution of protease inhibitors, and the protein was dialyzed against the same solution and clarified at 46,000*g*. The protein solution was applied to a DEAE-Sephacel column (Amersham Pharmacia Biotech, Uppsala, Sweden) preequilibrated with Solution A and bound proteins eluted with a linear gradient of KCl (10–500 mM). Pooled protein fractions were dialyzed against Solution B (10 mM Tris-HCl, pH 8.0, 0.2 mM EGTA, 0.01% NaN_3, 1 mM DTT, and 1:200 protease inhibitors) and applied to a Cibacron Blue 3G-A column (Sigma-Aldrich, St. Louis, MO) preequilibrated with Solution B. Bound proteins were eluted with the same buffer containing 2 M KCl and 1 mM ATP. Pooled protein fractions were dialyzed against Solution C (10 mM Tris-HCl, pH 8.0, 140 mM KCl, 0.01% NaN_3, 1 mM DTT, and 1:200 protease inhibitors), and applied to a Q-Sepharose column (Amersham Pharmacia Biotech) preequilibrated with Solution C. Bound proteins were eluted with a linear gradient of KCl (140–500 mM). The purified VLN1 was dialyzed against Buffer G (2 mM Tris-HCl, pH 8.0, 0.01% NaN_3, 0.2 mM $CaCl_2$, 0.2 mM ATP, and 0.2 mM DTT), aliquoted, frozen in liquid nitrogen, and stored at −80°C. VLN1 concentrations were determined by Bradford assay (Bio-Rad, Hercules, CA) with BSA as a standard.

Arabidopsis ADF1, maize (*Zea mays*) PROFILIN5 (ZmPRO5), and Arabidopsis FIM1 were purified as described previously (Carlier et al., 1997; Kovar et al., 2000a, 2000b). GS plasmid was kindly provided by T. Pollard (Yale University). Recombinant GS was purified from bacterial cells roughly according to Pope et al. (1997) initially with DEAE-Sepharose and further purified by Cibacron Blue 3G-A.

Actin was purified from rabbit skeletal muscle acetone powder (Spudich and Watt, 1971), and monomeric Ca-ATP-actin was purified by Sephacryl S-300 chromatography (Pollard, 1984) in G buffer (5 mM Tris-HCl, pH 8, 0.2 mM ATP, 0.1 mM $CaCl_2$, 0.5 mM DTT, and 0.1 mM azide). Actin was labeled on Cys-374 with pyrene iodoacetamide (Pollard, 1984). Maize pollen actin was purified according to Ren et al. (1997). Actin concentration was determined by spectrometry assuming an A_{290} for a 1 mg/mL solution of 0.63.

High-Speed and Low-Speed Cosedimentation Assays

High- and low-speed cosedimentation assays were used to examine the actin binding and actin-bundling properties of VLN1, respectively (Kovar et al., 2000b). All proteins were preclarified at 140,000*g* before an experiment. In a 200-μL reaction volume either 3.0 μM G-actin alone, 1.0 μM VLN1 alone, or G-actin with VLN1 was incubated in 1× F-buffer (10× stock: 50 mM Tris-HCl, pH 7.5, 5 mM DTT, 5 mM ATP, 1 M KCl, and 50 mM $MgCl_2$) in the presence of 1.0 mM EGTA (added from a 100-mM stock in 1× F-buffer). The final concentration of free calcium, [Ca^{2+}], was 4.6 nM. Free Ca^{2+} was calculated with EGTA software by Petesmif (PM Smith, University of Liverpool, UK), available at http://www.liv.ac.uk/luds/people/cds/bds/pms/cal.htm/. After a 90-min incubation at 22°C, samples were centrifuged at either 200,000*g* for 1 h in a TL-100 centrifuge (Beckman, Palo Alto, CA) at 4°C, or 13,500*g* for 30 min in a microcentrifuge at 4°C. After the supernatant was removed, protein sample buffer was added to the supernatant and the pellet. Equal amounts of pellet and supernatant samples were separated by 12.5% SDS-PAGE and stained with Coomassie Brilliant Blue R (Sigma-Aldrich).

High- and low-speed cosedimentation experiments were also used to determine the effect of varying [Ca^{2+}] on actin binding and bundling activities of VLN1. In these experiments, either 1.0 μM VLN1 alone, 3.0 μM actin alone, or 1.0 μM VLN1 with 3.0 μM actin was incubated in 1× F-buffer (200 μL total reaction volume) in the presence of 4.6 nM, 100 nM, 1.0 μM, 12 μM, or 1.0 mM free Ca^{2+} for 90 min at 22°C. After 80 μL was removed and added to 20 μL of 5× protein sample buffer (total protein; T), the remaining 120 μL was centrifuged as described above. Supernatant (80 μL) was removed and added to 20 μL 5× protein sample buffer. After removal of residual supernatant, the pellets were resuspended in 50 μL 2× protein sample buffer. Equal amounts of total protein (12 μL), supernatant (12 μL), and pellet (4 μL) were separated by 12.5% SDS-PAGE and stained with Coomassie Brilliant Blue R. Gels were scanned, and the intensity of bands was determined with IMAGEQUANT software (Personal Densitometer; Molecular Dynamics, Sunnyvale, CA). Actin and VLN1 from total protein lanes served as internal controls for gel loading. To determine a dissociation constant (K_d) (Kovar et al., 2000b), increasing amounts (0.3, 0.5, 0.8, 1.2, 1.8, 2.4, 2.6, 3.0, and 3.4 μM) of VLN1 or FIM1 were incubated with 3.0 μM preassembled F-actin for 60 min at 22°C. The samples were centrifuged at 200,000*g* for 1 h. The amount of VLN1 and FIM1 in the pellets or supernatant was quantified by scanning Coomassie-stained gels, using known amounts of VLN1 and FIM1 to generate standard curves. A K_d value for VLN1 and FIM1 bound to actin was calculated by fitting the data of protein bound versus protein free to a hyperbolic function with Kaleidagraph v3.6 software (Synergy Software, Reading, PA).

Nucleation Assay

Actin nucleation was performed essentially as described by Schafer et al. (1996). Monomeric actin at 2 μM (5% pyrene labeled) was incubated with VLN1 or GS for 5 min in Buffer G. Fluorescence of pyrene-actin was monitored with a PTI Quantamaster spectrofluorimeter (QM-2000-SE; Photon Technology International, South Brunswick, NJ) after the addition of 1/10 volume of 10× KMEI (1× contains 50 mM KCl, 1 mM $MgCl_2$, 1 mM EGTA, and 10 mM imidazole-HCl, pH 7.0).

Capping of Actin Filament Ends

Various concentrations of VLN1 or GS were incubated with 0.4 μM preformed actin filaments in KMEI supplemented with 0.2 mM ATP, 0.2 mM $CaCl_2$, 0.5 mM DTT, and 3 mM NaN_3 for 5 min at room temperature. The final free [Ca^{2+}] was 1 μM. The reaction mixture was supplemented with 1 μM G-actin (5% pyrene labeled) saturated by 4 μM human profilin 1 to initiate actin elongation at barbed ends.

Kinetics Studies of Actin Polymerization and Depolymerization

Polymerization of actin in the presence of VLN1 and ADF1 was measured by changes in pyrene fluorescence using a fluorescence spectrophotometer (model Safas Xenius, Safas SA, Monaco). Depolymerization of actin filaments was performed roughly as described by Huang et al. (2004). F-actin at 2.5 μM (40–50% pyrene labeled) was depolymerized by addition of an equimolar amount of ZmPRO5, in the presence or absence of VLN1 or GS. The decrease in pyrene fluorescence accompanying actin depolymerization was monitored for 800 s after addition of profilin. The final free [Ca^{2+}] was 10 μM for all reactions. For ADF induced depolymerization assay, F-actin was depolymerized by addition of 0.6 μM ADF1 and/or 8 μM latrunculin B. To test the effect of VLN1, F-actin was preincubated with VLN1 for 5 min at room temperature. The decrease of pyrene fluorescence was monitored after addition of ADF and/or latrunculin B.

Light Scattering Assay to Measure Bundling Activity

A kinetic light scattering assay was performed to determine the ability of VLN1 to form actin bundles during polymerization. Light scattering was monitored by 90° light scattering of unlabeled actin at 400 nm. The change of light scattering was recorded after addition of polymerization salts to VLN1 and G-actin solutions.

Fluorescence Microscopy of Actin Filaments

Individual actin filaments labeled with fluorescent phalloidin were imaged by fluorescence microscopy according to Blanchoin et al. (2000a, 2000b). Actin at 4 μM alone, or together with VLN1, was polymerized in 50 mM KCl, 1 mM $MgCl_2$, 1 mM EGTA, 0.2 mM ATP, 0.2 mM $CaCl_2$, 0.5 mM DTT, 3 mM NaN_3, and 10 mM imidazole, pH 7.0, at 25°C for 30 min and labeled with an equimolar amount of rhodamine-phalloidin (Sigma-Aldrich) during polymerization. The polymerized F-actin was diluted to 10 nM in fluorescence buffer containing 10 mM imidazole, pH 7.0, 50 mM KCl, 1 mM $MgCl_2$, 100 mM DTT, 100 μg/mL glucose oxidase, 15 mg/mL glucose, 20 μg/mL catalase, and 0.5% methylcellulose. A dilute sample of 3 μL was applied to a 22 × 22-mm cover slip coated with poly-L-lysine (0.01%). Actin filaments were observed by epifluorescence illumination under a Nikon Microphot SA microscope (Tokyo, Japan) equipped with a 60×, 1.4 NA Planapo objective and digital images were collected with a Hamamatsu ORCA-ER 12-bit CCD camera (Hamamatsu Photonics, Hamamatsu City, Japan) using Metamorph (version 6.0) software (Universal Imaging, Downingtown, PA).

ACKNOWLEDGMENTS

We gratefully acknowledge the help and advice of colleagues in the Staiger lab and the Purdue Motility Group (www.bio.purdue.edu/pmg/). Special thanks are due to Faisal Chaudhry (Purdue University, West Lafayette, IN) for providing purified plasma gelsolin, to Etsuo Yokota and Teruo Shimmen (University of Hyogo, Japan) for suggesting the experiments with calcium–calmodulin and sharing their unpublished data, and to Jörg Becker and José Feijó (Instituto Gulbenkian, Oeiras, Portugal) for providing pollen microarray data. This work was supported with grants from the U.S. National Science Foundation (0130576-MCB) and the U.S. Department of Energy–Biosciences Division (DE-FG02-04ER15526) to C.J.S. Support for L.B. was through an Actions Thématiques et Inicitatives sur Programmes et Equipes from the Centre Naitonal de la Recherche Scientifique and for R.C.R. from the Swedish Medical Science Research Council. Microscopy facilities were established with partial financial support from the U.S. National Science Foundation (0217552-DBI).

Received October 13, 2004; accepted December 2, 2004.

REFERENCES

Arpin, M., Pringault, E., Finidori, J., Garcia, A., Jeltsch, J.-M., Vandekerckhove, J., and Louvard, D. (1988). Sequence of human villin: A large duplicated domain homologous with other actin-severing proteins and a unique small carboxy-terminal domain related to villin specificity. J. Cell Biol. **107,** 1759–1766.

Baluska, F., Busti, E., Dolfini, S., Gavazzi, G., and Volkmann, D. (2001). *Lilliputian* mutant of maize lacks cell elongation and shows defects in organization of actin cytoskeleton. Dev. Biol. **236,** 478–491.

Bazari, W.L., Matsudaira, P., Wallek, M., Smeal, T., Jakes, R., and Ahmed, Y. (1988). Villin sequence and peptide map identify six homologous domains. Proc. Natl. Acad. Sci. USA **85,** 4986–4990.

Bernstein, B.W., and Bamburg, J.R. (1982). Tropomyosin binding to F-actin protects the F-actin from disassembly by brain actin-depolymerizing factor (ADF). Cell Motil. Cytoskeleton **2,** 1–8.

Blanchoin, L., Amann, K.J., Higgs, H.N., Marchand, J.-B., Kaiser, D.A., and Pollard, T.D. (2000b). Direct observation of dendritic actin filament networks nucleated by Arp2/3 complex and WASP/Scar proteins. Nature **404,** 1007–1011.

Blanchoin, L., and Pollard, T.D. (1999). Mechanism of interaction of *Acanthamoeba* actophorin (ADF/cofilin) with actin filaments. J. Biol. Chem. **274,** 15538–15546.

Blanchoin, L., Pollard, T.D., and Hitchcock-DeGregori, S.E. (2001). Inhibition of the Arp2/3 complex-nucleated actin polymerization and branch formation by tropomyosin. Curr. Biol. **11,** 1300–1304.

Blanchoin, L., Pollard, T.D., and Mullins, R.D. (2000a). Interactions of ADF/cofilin, Arp2/3 complex, capping protein and profilin in remodeling of branched actin filament networks. Curr. Biol. **10,** 1273–1282.

Bretscher, A., and Weber, K. (1979). Villin: The major microfilament-associated protein of the intestinal microvillus. Proc. Natl. Acad. Sci. USA **76,** 2321–2325.

Bretscher, A., and Weber, K. (1980). Villin is a major protein of the microvillus cytoskeleton which binds both G and F actin in a calcium-dependent manner. Cell **20,** 839–847.

Broschat, K.O., Weber, A., and Burgess, D.R. (1989). Tropomyosin stabilizes the pointed end of actin filaments by slowing depolymerization. Biochemistry **28,** 8501–8506.

Burtnick, L.D., Koepf, E.K., Grimes, J., Jones, E.Y., Stuart, D.I., McLaughlin, P.J., and Robinson, R.C. (1997). The crystal structure of plasma gelsolin: Implications for actin severing, capping, and nucleation. Cell **90,** 661–670.

Burtnick, L.D., Urosev, D., Irobi, E., Narayan, K., and Robinson, R.C. (2004). Structure of the N-terminal half of gelsolin bound to actin: Roles in severing, apoptosis and FAF. EMBO J. **23,** 2713–2722.

Carlier, M.-F., Laurent, V., Santolini, J., Melki, R., Didry, D., Xia, G.-X., Hong, Y., Chua, N.-H., and Pantaloni, D. (1997). Actin depolymerizing factor (ADF/cofilin) enhances the rate of filament turnover: Implication in actin-based motility. J. Cell Biol. **136,** 1307–1322.

Chen, C.Y., Wong, E.I., Vidali, L., Estavillo, A., Hepler, P.K., Wu, H.-m., and Cheung, A.Y. (2002). The regulation of actin organization by actin-depolymerizing factor in elongating pollen tubes. Plant Cell **14,** 2175–2190.

Choe, H., Burtnick, L.D., Mejillano, M., Yin, H.L., Robinson, R.C., and Choe, S. (2002). The calcium activation of gelsolin: Insights from the 3 Å structure of the G4–G6/actin complex. J. Mol. Biol. **324,** 691–702.

Dong, C.-H., Xia, G.-X., Hong, Y., Ramachandran, S., Kost, B., and Chua, N.-H. (2001). ADF proteins are involved in the control of flowering and regulate F-actin organization, cell expansion, and organ growth in Arabidopsis. Plant Cell **13,** 1333–1346.

Drøbak, B.K., Franklin-Tong, V.E., and Staiger, C.J. (2004). Tansley review: The role of the cytoskeleton in plant cell signaling. New Phytol. **163,** 13–30.

El-Assal, S.E.-D., Le, J., Basu, D., Mallery, E.L., and Szymanski, D.B. (2004). *DISTORTED2* encodes an ARPC2 subunit of the putative *Arabidopsis* ARP2/3 complex. Plant J. **38,** 526–538.

Fan, X., Hou, J., Chen, X., Chaudhry, F., Staiger, C.J., and Ren, H. (2004). Identification and characterization of a Ca^{2+}-dependent actin-filament severing protein from lily pollen. Plant Physiol. **136,** 3979–3989.

Ferrary, E., et al. (1999). In vivo, villin is required for Ca^{2+}-dependent F-actin disruption in intestinal brush borders. J. Cell Biol. **146,** 819–829.

Friederich, E., and Louvard, D. (1999). Villin. In Guidebook to the Cytoskeletal and Motor Proteins, T. Kries and R. Vale, eds (New York: Oxford University Press), pp. 175–179.

Friederich, E., Vancompernolle, K., Louvard, D., and Vandekerckhove, J. (1999). Villin function in the organization of the actin cytoskeleton. Correlation of *in vivo* effects to its biochemical activities in vitro. J. Biol. Chem. **274,** 26751–26760.

Fu, Y., Wu, G., and Yang, Z. (2001). Rop GTPase-dependent dynamics of tip-localized F-actin controls tip growth in pollen tubes. J. Cell Biol. **152,** 1019–1032.

Glenney, J.R.J., and Weber, K. (1981). Calcium control of microfilaments: Uncoupling of the F-actin-severing and -bundling activity of villin by limited proteolysis *in vitro*. Proc. Natl. Acad. Sci. USA **78,** 2810–2814.

Glenney, J.R.J., Bretscher, A., and Weber, K. (1980). Calcium control of the intestinal microvillus cytoskeleton: Its implications for the regulation of microfilament organizations. Proc. Natl. Acad. Sci. USA **77,** 6458–6462.

Glenney, J.R.J., Geisler, N., Kaulfus, P., and Weber, K. (1981). Demonstration of at least two different actin-binding sites in villin, a calcium-regulated modulator of F-actin organization. J. Biol. Chem. **256,** 8156–8161.

Gross, P., Julius, C., Schmelzer, E., and Hahlbrock, K. (1993). Translocation of cytoplasm and nucleus to fungal penetration sites is associated with depolymerization of microtubules and defence gene activation in infected, cultured parsley cells. EMBO J. **12,** 1735–1744.

Heintzelman, M.B., and Mooseker, M.S. (1992). Assembly of the intestinal brush border cytoskeleton. Curr. Top. Dev. Biol. **26,** 93–122.

Hesterberg, L.K., and Weber, K. (1983). Demonstration of three distinct calcium-binding sites in villin, a modulator of actin assembly. J. Biol. Chem. **258,** 365–369.

Holdaway-Clarke, T.L., and Hepler, P.K. (2003). Control of pollen tube growth: Role of ion gradients and fluxes. New Phytol. **159,** 539–563.

Hopmann, R., and Miller, K.G. (2003). A balance of capping protein and profilin functions is required to regulate actin polymerization in *Drosophila* bristle. Mol. Biol. Cell **14,** 118–128.

Huang, S., Blanchoin, L., Chaudhry, F., Franklin-Tong, V.E., and Staiger, C.J. (2004). A gelsolin-like protein from *Papaver rhoeas* pollen (PrABP80) stimulates calcium-regulated severing and depolymerization of actin filaments. J. Biol. Chem. **279,** 23364–23375.

Huang, S., Blanchoin, L., Kovar, D.R., and Staiger, C.J. (2003). *Arabidopsis* capping protein (AtCP) is a heterodimer that regulates assembly at the barbed ends of actin filaments. J. Biol. Chem. **278,** 44832–44842.

Hussey, P.J., Allwood, E.G., and Smertenko, A.P. (2002). Actin-binding proteins in the *Arabidopsis* genome database: Properties of functionally distinct plant actin-depolymerizing factors/cofilins. Philos. Trans. R. Soc. Lond. B Biol. Sci. **357,** 791–798.

Janmey, P.A., and Matsudaira, P.T. (1988). Functional comparison of villin and gelsolin. Effects of Ca^{2+}, KCl, and polyphosphoinositides. J. Biol. Chem. **263,** 16738–16743.

Ketelaar, T., Faivre-Moskalenko, C., Esseling, J.J., de Ruijter, N.C.A., Grierson, C.S., Dogterom, M., and Emons, A.M.C. (2002). Positioning of nuclei in Arabidopsis root hairs: An actin-regulated process of tip growth. Plant Cell **14,** 2941–2955.

Klahre, U., Friederich, E., Kost, B., Louvard, D., and Chua, N.-H. (2000). Villin-like actin-binding proteins are expressed ubiquitously in Arabidopsis. Plant Physiol. **122,** 35–47.

Kobayashi, I., Kobayashi, Y., Yamaoka, N., and Kunoh, H. (1992). Recognition of a pathogen and a nonpathogen by barley coleoptile cells. III. Responses of microtubules and actin filaments in barley coleoptile cells to penetration attempts. Can. J. Bot. **70,** 1815–1823.

Kobayashi, Y., Kobayashi, I., Funaki, Y., Fujimoto, S., Takemoto, T., and Kunoh, H. (1997). Dynamic reorganization of microfilaments and microtubules is necessary for the expression of non-host resistance in barley coleoptile cells. Plant J. **11,** 525–537.

Kovar, D.R., Drøbak, B.K., and Staiger, C.J. (2000a). Maize profilin isoforms are functionally distinct. Plant Cell **12,** 583–598.

Kovar, D.R., Staiger, C.J., Weaver, E.A., and McCurdy, D.W. (2000b). AtFim1 is an actin filament crosslinking protein from *Arabidopsis thaliana*. Plant J. **24,** 625–636.

Kumar, N., and Khurana, S. (2004). Identification of a functional switch for actin severing by cytoskeletal proteins. J. Biol. Chem. **279,** 24915–24918.

Kumar, N., Tomar, A., Parrill, A.L., and Khurana, S. (2004). Functional dissection and molecular characterization of calcium-sensitive actin-capping and actin-depolymerizing sites in villin. J. Biol. Chem. **279,** 45036–45046.

Le, J., El-Din El-Assal, S., Basu, D., Saad, M.E., and Szymanski, D.B. (2003). Requirements for an *Arabidopsis ATARP2* and *ATARP3* during development. Curr. Biol. **13,** 1341–1347.

Lopez, I., Anthony, R.G., Maciver, S.K., Jiang, C.-J., Khan, S., Weeds, A.G., and Hussey, P.J. (1996). Pollen specific expression of maize genes encoding actin depolymerizing factor-like proteins. Proc. Natl. Acad. Sci. USA **93,** 7415–7420.

Maciver, S.K., and Hussey, P.J. (2002). The ADF/cofilin family: Actin-remodeling proteins. Genome Biol. **3,** 3007.3001–3007.3012.

Maciver, S.K., Zot, H.G., and Pollard, T.D. (1991). Characterization of actin filament severing by actophorin from *Acanthamoeba castellanii*. J. Cell Biol. **115,** 1611–1620.

Mahajan-Miklos, S., and Cooley, L. (1994). The villin-like protein encoded by the Drosophila quail gene is required for actin bundle assembly during oogenesis. Cell **78,** 291–301.

Markus, M.A., Matsudaira, P., and Wagner, G. (1997). Refined structure of villin 14T and a detailed comparison with other actin-severing domains. Protein Sci. **6,** 1197–1209.

Matova, N., Mahajan-Miklos, S., Mooseker, M.S., and Cooley, L. (1999). *Drosophila* Quail, a villin-related protein, bundles actin filaments in apoptotic nurse cells. Development **126,** 5645–5657.

Matsudaira, P.T., and Burgess, D.R. (1979). Identification and organization of the components in the isolated microvillus cytoskeleton. J. Cell Biol. **83,** 667–673.

McCurdy, D.W., Kovar, D.R., and Staiger, C.J. (2001). Actin and actin-binding proteins in higher plants. Protoplasma **215,** 89–104.

Nagai, R., and Rebhun, L.I. (1966). Cytoplasmic microfilaments in streaming *Nitella* cells. J. Ultrastruct. Res. **14,** 571–589.

Nakayasu, T., Yokota, E., and Shimmen, T. (1998). Purification of an actin-binding protein composed of 115-kDa polypeptide from pollen tubes of lily. Biochem. Biophys. Res. Commun. **249,** 61–65.

Nishida, E., Muneyuki, E., Maekawa, S., Ohta, Y., and Sakai, H. (1985). An actin-depolymerizing protein (destrin) from porcine kidney. Its action on F-actin containing or lacking tropomyosin. Biochemistry **24,** 6624–6630.

Northrop, J., Weber, A., Mooseker, M.S., Franzini-Armstrong, C., Bishop, M.F., Dubyak, G.R., Tucker, M., and Walsh, T.P. (1986). Different calcium dependence of the capping and cutting activities of villin. J. Biol. Chem. **261,** 9274–9281.

Pollard, T.D. (1984). Polymerization of ADP-actin. J. Cell Biol. **99,** 769–777.

Pollard, T.D., and Cooper, J.A. (1984). Quantitative analysis of the effect of *Acanthamoeba* profilin on actin filament nucleation and elongation. Biochemistry **23,** 6631–6641.

Pollard, T.D., Blanchoin, L., and Mullins, R.D. (2000). Molecular mechanisms controlling actin filament dynamics in nonmuscle cells. Annu. Rev. Biophys. Biomol. Struct. **29,** 545–576.

Pope, B., Gooch, J.T., and Weeds, A.G. (1997). Probing the effects of calcium on gelsolin. Biochemistry **36,** 15848–15855.

Pope, B., Way, M., Matsudaira, P.T., and Weeds, A. (1994). Characterisation of the F-actin binding domains of villin: Classification of F-actin binding proteins into two groups according to their binding sites on actin. FEBS Lett. **338,** 58–62.

Ren, H., Gibbon, B.C., Ashworth, S.L., Sherman, D.M., Yuan, M., and Staiger, C.J. (1997). Actin purified from maize pollen functions in living plant cells. Plant Cell **9,** 1445–1457.

Ressad, F., Didry, D., Xia, G.-X., Hong, Y., Chua, N.-H., Pantaloni, D., and Carlier, M.-F. (1998). Kinetic analysis of the interaction of actin-depolymerizing factor (ADF)/cofilin with G- and F-actins. Comparison of plant and human ADFs and effect of phosphorylation. J. Biol. Chem. **273,** 20894–20902.

Robinson, R.C., Mejillano, M., Le, V.P., Burtnick, L.D., Yin, H.L., and Choe, S. (1999). Domain movement in gelsolin: A calcium-activated switch. Science **286,** 1939–1942.

Schafer, D.A., Jennings, P.B., and Cooper, J.A. (1996). Dynamics of capping protein and actin assembly in vitro: Uncapping barbed ends by polyphosphoinositides. J. Cell Biol. **135,** 169–179.

Schmelzer, E. (2002). Cell polarization, a crucial process in fungal defence. Trends Plant Sci. **7,** 411–415.

Shimmen, T., and Yokota, E. (2004). Cytoplasmic streaming in plants. Curr. Opin. Cell Biol. **16,** 68–72.

Shimmen, T., Hamatani, M., Saito, S., Yokota, E., Mimura, T., Fusetani, N., and Karaki, H. (1995). Roles of actin filaments in cytoplasmic streaming and organization of transvacuolar strands in root hair cells of *Hydrocharis*. Protoplasma **185,** 188–193.

Smertenko, A.P., Allwood, E.G., Khan, S., Jiang, C.-J., Maciver, S.K., Weeds, A.G., and Hussey, P.J. (2001). Interaction of pollen-specific actin-depolymerizing factor with actin. Plant J. **25,** 203–212.

Spudich, J.A., and Watt, S. (1971). The regulation of rabbit skeletal muscle contraction. I. Biochemical studies of the interaction of the tropomyosin-troponin complex with actin and the proteolytic fragments of myosin. J. Biol. Chem. **246,** 4866–4871.

Staiger, C.J. (2000). Signaling to the actin cytoskeleton in plants. Annu. Rev. Plant Physiol. Plant Mol. Biol. **51,** 257–288.

Staiger, C.J., and Hussey, P.J. (2004). Actin and actin-modulating proteins. In The Plant Cytoskeleton in Cell Differentiation and Development, P.J. Hussey, ed (Oxford: Blackwell Publishers), pp. 32–80.

Staiger, C.J., Yuan, M., Valenta, R., Shaw, P.J., Warn, R.M., and Lloyd, C.W. (1994). Microinjected profilin affects cytoplasmic streaming in plant cells by rapidly depolymerizing actin microfilaments. Curr. Biol. **4,** 215–219.

Thimann, K.V., Reese, K., and Nachmias, V.T. (1992). Actin and the elongation of plant cells. Protoplasma **171,** 153–166.

Tilney, L.G., Connelly, P.S., Ruggiero, L., Vranich, K.A., and Guild, G.M. (2003). Actin filament turnover regulated by cross-linking accounts for the size, shape, location, and number of actin bundles in *Drosophila* bristles. Mol. Biol. Cell **14,** 3953–3966.

Tominaga, M., Yokota, E., Vidali, L., Sonobe, S., Hepler, P.K., and Shimmen, T. (2000). The role of plant villin in the organization of the actin cytoskeleton, cytoplasmic streaming and the architecture of the transvacuolar strand in root hair cells of *Hydrocharis*. Planta **210,** 836–843.

Valster, A.H., Pierson, E.S., Valenta, R., Hepler, P.K., and Emons, A.M.C. (1997). Probing the plant actin cytoskeleton during cytokinesis and interphase by profilin microinjection. Plant Cell **9,** 1815–1824.

Vidali, L., Yokota, E., Cheung, A.Y., Shimmen, T., and Hepler, P.K. (1999). The 135 kDa actin-bundling protein from *Lilium longiflorum* pollen is the plant homologue of villin. Protoplasma **209,** 283–291.

Vignjevic, D., Yarar, D., Welch, M.D., Peloquin, J., Svitkina, T., and Borisy, G.G. (2003). Formation of filopodia-like bundles in vitro from a dendritic network. J. Cell Biol. **160,** 951–962.

Waller, F., and Nick, P. (1997). Response of actin microfilaments during phytochrome-controlled growth of maize seedlings. Protoplasma **200,** 154–162.

Waller, F., Riemann, M., and Nick, P. (2002). A role for actin-driven secretion in auxin-induced growth. Protoplasma **219,** 72–81.

Wasteneys, G.O., and Galway, M.E. (2003). Remodeling the cytoskeleton for growth and form: An overview with some new views. Annu. Rev. Plant Biol. **54,** 691–722.

Yamashiro, S., Kameyama, K., Kanzawa, N., Tamiya, T., Mabuchi, I., and Tsuchiya, T. (2001). The gelsolin/fragmin family protein identified in the higher plant *Mimosa pudica*. J. Biochem. **130,** 243–249.

Yin, H.L. (1999). Gelsolin. In Guidebook to the Cytoskeletal and Motor Proteins, T. Kreis and R. Vale, eds (New York: Oxford University Press), pp. 99–102.

Yokota, E., and Shimmen, T. (1999). The 135-kDa actin-bundling protein from lily pollen tubes arranges F-actin into bundles with uniform polarity. Planta **209,** 264–266.

Yokota, E., and Shimmen, T. (2000). Characterization of native actin-binding proteins from pollen: Myosin and the actin-bundling proteins, 135-ABP and 115-ABP. In Actin: A Dynamic Framework for Multiple Plant Cell Functions, C.J. Staiger, F. Baluska, D. Volkmann, and P. Barlow, eds (Dordrecht, The Netherlands: Kluwer Academic Publishers), pp. 103–118.

Yokota, E., Muto, S., and Shimmen, T. (2000). Calcium-calmodulin suppresses the filamentous actin-binding activity of 135-kilodalton actin-bundling protein isolated from lily pollen tubes. Plant Physiol. **123,** 645–654.

Yokota, E., Takahara, K.-i., and Shimmen, T. (1998). Actin-bundling protein isolated from pollen tubes of lily. Plant Physiol. **116,** 1421–1429.

Yokota, E., Vidali, L., Tominaga, M., Tahara, H., Orii, H., Morizane, Y., Hepler, P.K., and Shimmen, T. (2003). Plant 115-kDa actin-filament bundling protein, P-115-ABP, is a homologue of plant villin and is widely distributed in cells. Plant Cell Physiol. **44,** 1088–1099.

Zimmermann, P., Hirsch-Hoffmann, M., Hennig, L., and Gruissem, W. (2004). GENEVESTIGATOR. Arabidopsis microarray database and analysis toolbox. Plant Physiol. **136,** 2621–2632.